

A  
*Dissertation Report*  
On  
**MOLECULAR INSIGHTS INTO THE INTERACTION OF A SMALL  
MOLECULE INHIBITOR WITH  
β- SECRETASE (BACE1) ENZYME: A MOLECULAR DYNAMICS  
SIMULATION STUDY**

Submitted in partial fulfillment of the requirement for the award of the degree of

**MASTER OF SCIENCE**

**IN**

**CHEMISTRY**

*Submitted by*

**Manjinder Kaur**  
**(Reg. No.: 301602026)**

*Under the supervision of*  
**Dr. Bhupesh Goyal**

*Assistant Professor*  
School of Chemistry and Biochemistry



**THAPAR INSTITUTE**  
OF ENGINEERING & TECHNOLOGY  
(Deemed to be University)

**SCHOOL OF CHEMISTRY AND BIOCHEMISTRY**  
**THAPAR INSTITUTE OF ENGINEERING & TECHNOLOGY**

(Deemed to be University)

**PATIALA-147004 (INDIA)**

(July 2018)

## CERTIFICATE

This is to certify that the dissertation entitled, "**Molecular insights into the interaction of a small molecule inhibitor with  $\beta$ -secretase (BACE1) enzyme: A molecular dynamics simulation study**" being submitted by Manjinder Kaur in partial fulfillment of the requirements for the award of degree of Masters of Science in chemistry to the School of Chemistry and Biochemistry, Thapar Institute of Engineering & Technology, Patiala is a bonafide work carried by her under my supervision. The contents of this dissertation have not been submitted for the award of any other degree or diploma.

*Bhupesh Goyal*  
3/8/2018

Dr. Bhupesh Goyal

Assistant professor

School of Chemistry and Biochemistry

Thapar Institute of Engineering & Technology, Patiala-147004

## Declaration

I hereby declare that the work being presented in the dissertation entitled "**Molecular insights into the interaction of a small molecule inhibitor with  $\beta$ -secretase (BACE1) enzyme: A molecular dynamics simulation study**" in the partial fulfillment of the requirements for the award of the Degree of Master of Science in Chemistry, and being submitted to the School of Chemistry and Biochemistry, Thapar Institute of Engineering & Technology Patiala. This is my own work during the period of January to July 2018, under the supervision of **Dr. Bhupesh Goyal** (School of Chemistry and Biochemistry). I have not submitted the contents embodied in this dissertation for the award of any other degree.

Place: *Patiala*

Waninder Kaur *Manjinder kaur*

Date: *3-Aug-2018*

This is to certify that the statement made by the candidate is correct and true to the best of our knowledge.

*Bhupesh Goyal*

Dr. Bhupesh Goyal

Assistant Professor

School of Chemistry & Biochemistry

Thapar Institute of Engineering Technology

Patiala 147004

## **Acknowledgement**

The writing of this dissertation has been one of the most significant academic challenges I have ever had to face. Without the support, patience and guidance of the following people, this study would not have been completed. It is to them that I owe my deepest gratitude.

First of all I express my sincere gratitude to my supervisor **Dr. Bhupesh Goyal** for his guidance and encouragement throughout the course of this work.

I would like to express my sincere thanks to **Dr. Amjad** Ali, Head SCBC, Thapar Institute and Engineering and Technology, Patiala, for providing the necessary facilities needed for this work and directly or indirectly encouraged me to do the work.

I express words of thanks from the bottom of my heart to the Ph.D. scholars Simranjeet Singh, Mrs. Suniba, Rajneet Saini for their cordial support and valuable information which helped me in completing this task through various stages.

At last, but not the least I must express my very profound gratitude to my parents and to my friends for providing me with unfailing support and continuous encouragement throughout my years of study and through the process of researching and writing this thesis. And finally thanks to God who made all the things possible.

I am very thankful to everyone who all supported me, for I have completed my thesis effectively and moreover, on time.

**(Manjinder Kaur)**

## Abstract

AD is a neurodegenerative, irreversible and progressive diseases. It is the most common cause of dementia affecting over 40 million people worldwide, but still there is no proper cure for this disease till now. According to World Alzheimer's, report 2018 the rate of AD enhanced by three times approximately by 2050. One of the major characteristics and chronic marks of AD is shown by the senile plaques and neurofibrillary tangles. These plaques and tangles affect the activity of brain or kills brain cells. A $\beta$  peptides were derived from amyloid precursor protein (APP) by the cleavage of  $\beta$ -secretase (BACE-1),  $\gamma$ -secretase enzymes and BACE-1 participates in the rate-limiting step in A $\beta$  production. Thus BACE1 is an important target for the development of anti-Alzheimer's agents along with A $\beta$  peptide. In the present study reported inhibitor PF-06751979 (**C1**) was selected to get insight into the inhibitory mechanism against BACE-1 using *in silico* studies. The Results of the study, shows significant reduction in the fluctuation in loop regions, i.e. insert-A (Phe159-Leu167), insert-B (Lys218-Asn221), insert-C (Ala251-Pro258), insert-D (Trp270-Gly273), insert-E (Glu290-Ser295) and insert-F (Gln316-Asp318) as compare to apo-BACE1. Interactions results also shoe the interactions with the active pocket residues of BACE-1 i.e. S1 (Gln73 and Phe108), S1' (Thr72), S2 (Asn233), S3 (Ile110) and S4 (Gln73 and Thr232). Results also show the interactions with flap residues (Gly66-Glu77) which confirms the strong binding with flap and keep the flap in close confirmation in the presence of **C1**. The molecular insights from the present study will help in the rational design of more potent drug molecules against AD.

# Contents

<b>List of figures</b>	vii-viii
<b>List of Tables</b>	ix
<b>List of Abbreviations and Symbols</b>	x
<b>Chapter 1: Introduction</b>	1-10
1.1 Protein folding	
1.2 Mechanism of protein folding	
1.2.1 Primary structure	
1.2.2 Secondary structure	
1.2.3 Tertiary structure	
1.3 Alzheimer's diseases	
1.4 Causes of Alzheimer's diseases	
1.5 Beta-site amyloid precursor protein cleaving enzyme 1 (BACE-1)	
<b>Chapter 2: Computational details</b>	11-12
2.1 System preparation: A $\beta$ <sub>42</sub> monomer and protofibril structure	
2.2 Parameterization of C1	
2.3 Molecular docking	
2.4 Molecular dynamics simulation and analysis	
<b>Chapter 3: Literature Review</b>	13-16
<b>Chapter 4: Results and Discussion</b>	17-24
<b>Chapter 5: Conclusion</b>	25
<b>Chapter 6: Reference</b>	26-30

## List of figures

**Figure 1.1:** Free energy folding landscape for chaperone-mediated protein folding.

**Figure 1.2:** Condensation reaction between two generic amino acids. R1 and R2 indicate side chains of amino acids.

**Figure 1.3:** Ribbon diagram showing the solution structure of human interleukin8. The red spirals indicate  $\alpha$ -helices while the blue arrows show  $\beta$ -sheets. Both of these structures are components of a protein's secondary structure.

**Figure 1.4:** Worldwide dementia statistics.

**Figure 1.5:** cleavage of beta amyloid precursor proteins.

**Figure 1.6:** Chemical structure of first oral bioavailable BACE-1 inhibitors.

**Figure 1.7:** chemical structure of the non - substrate based BACE-1 inhibitors.

**Figure 1.8:** BACE-1 inhibitor PF-06751979 (64).

**Figure 4.1.** Cartoon representation of BACE1 enzyme (PDB ID: 1FKN) is shown in panel a. The 2D chemical structure of PF-06751979 (64 or C1) ligand is shown in panel b.

**Figure 4.2.** The best docked complex of BACE1 with C1 is shown in panel a& b. BACE1 is shown in the cartoon representation and ligand is shown in the stick representation. The 2D interaction maps of hydrophobic contacts of BACE1 residues are shown in red semicircles with BTT as shown in panel c. The 2D maps were generated using LigPlot+ software.

**Figure 4.3.** The radius-of-gyration ( $R_g$ ) of apo-BACE1 (black) and BACE1-C1 complex (red) during simulation.

**Figure 4.4.** The root-mean-square deviation (RMSD) of apo-BACE1 (black) and BACE1-C1 complex (red) during simulation.

**Figure 4.5.** The  $C\alpha$  root-mean-square fluctuation (RMSF) of each residue for apo-BACE1 and BACE1-C1 complex is shown in panel c.

**Figure 4.6.** The number of hydrogen bonds between BACE1 and C1 during simulation with value on the top of the graph indicates the total number of hydrogen bonds.

**Figure 4.7.** The snapshot of central member of top most cluster represent hydrogen bond interactions between BACE1 residues and C1 is shown in panel a. The time dependence of distance between Gln73, Thr232 and Asn233 is shown in panel b. The 2D interaction maps of

hydrophobic contacts of top most cluster of BACE1 residues are shown in red semicircles with **C1** as shown in panel c.

**Figure 4.8.** Snapshot of flap dynamics (panel a) and interatomic distance between C $\alpha$  Thr72 – C $\beta$  Asp32of flap region for apo-BACE1 (black) and BACE1-**C1**complex (red) during the course of simulation time (panel b).

**Figure 4.9.** Snapshot of flap dynamics (panel a) and interatomic distance between C $\alpha$  Tyr71 – C $\beta$  Asp32of flap region for apo-BACE1 (black) and BACE1-**C1**complex (red) during the course of simulation time (panel b).

## **List of tables**

**Table 4.1.** Molecular docking analysis of BACE-1 and C1 using Autodock.

## List of Abbreviations and Symbols

**AchE:** Acetyl Cholinesterase

**AD:** Alzheimer's Disease

**ApoE:** Apolipoprotein E

**APP:** Amyloid Precursor Protein

**A $\beta$ :** Amyloid beta

**AFM:** Atomic Force Microscopy

**ATB:** Automated Topology Builder

**ADT:** AutoDock Tools

**BACE1:**  $\beta$ -site Amyloid Precursor Protein Cleaving Enzyme 1

**CADD:** Computer-Assisted Drug Design

**EM:** Electron Microscopy

**FAD:** Familial Alzheimer's Disease

**GOLD:** Genetic Optimization for Ligand Docking

**GROMACS:** GRoningen MACHine for Chemical Simulations

**H-bonding:** Hydrogen-bonding

**hERG:** Human Ether-à-go-go-Related Gene

**LBDD:** Ligand-Based Drug Design

**NMR:** Nuclear Magnetic Resonance Spectroscopy

**PDB:** Protein Data Bank

**QSAR:** Quantitative Structure-Activity Relationship

**RMSD:** Root Mean Square Deviation

**SAXS:** Small Angle X-ray Scattering

**WT:** Wild-type

# CHAPTER-1

## Introduction

### 1.1 Protein folding

Protein folding is important biological process that helps the protein to function. Folding starts from high energy, high entropy state to low energy, low entropy. Unfolded protein has high entropy as it starts folding entropy decreases. In protein folding nascent protein is transformed into the native folded structure. The 3-dimensional structure defines the function of the protein [1]. There are a number of factors that help on developing protein folding and protein stability like hydrophobic contacts, hydrogen bonding and pi-pi interactions. But sometime protein leads to misfolding and causes lethal diseases like Alzheimer's diseases, amyotrophic lateral sclerosis, Huntington's diseases and Parkinson's diseases [2].

To explain the protein folding a landscape represents with different energy levels. The landscapes of 3-dimensional funnel was used to explain the protein folding. Conformation of protein depends on the free energy and it is due to interaction between amino acids, small changes in the surface of landscape results in new local free energy minima or different stable structures of protein, which may be resulted to protein aggregation [3]. The energy of folding landscapes depends upon protein concentration, temperature, pH, salt, and surfactants etc.

When protein aggregates are more stable than native state of proteins than aggregated states are trapped in the kinetically deepest valley of landscape. So, native state and aggregated state of proteins are different in their intermolecular and intramolecular interactions. Chaperones are protein control system and molecular chaperones play an important role in rearranging the structure formed by hydrophobic interaction [4]. Since protein folding starts from the molten globule state and leads to folded state through transition state. But sometimes the molten globule deviates from protein folding and then chaperones catalysis helps the protein to fold in the right manner. If chaperones failed to act as catalysis then protein form are prion protein, which are called misfolding protein [5].

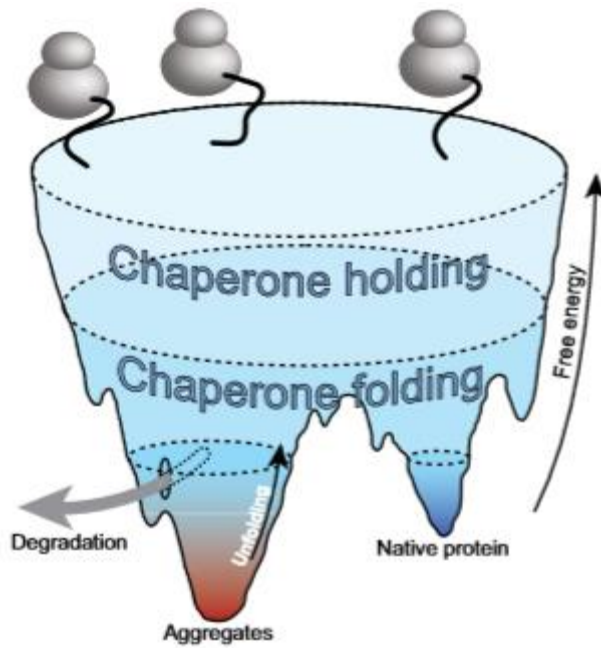


**Figure 1.1:** Free energy folding landscape for chaperone-mediated protein folding [6].

## 1.2 Mechanism of protein folding

The process of folding protein is deal with some steps:

**1.2.1 Primary structure:** The amino acids are origin of protein and primary structure is consisting of linear chains of amino acids. The first step in the formation of protein is the coding of amino acids in the form of linear chain connected by peptide bonds. The coding is essential in protein folding because it will determine the variety of interaction between amino acids in protein folding [7]. The primary structure contains charged or uncharged polar side chains (hydrophilic side chain) and non-polar side chain (hydrophobic side chain) in nature. Chemical and biological properties of proteins are not much depend on primary structure of proteins they are more dependent on tertiary structure of proteins [8].

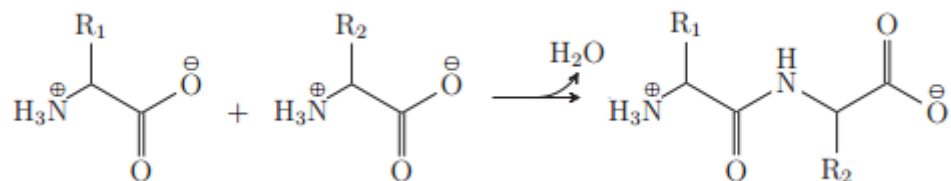


**Figure 1.2:** Condensation reaction between two generic amino acids. R1 and R2 indicate side chains of amino acids.

**1.2.2 Secondary structure:** Secondary structures are 3-dimensional in nature and they are non-functional. The secondary structures are consists of  $\alpha$ -helix and  $\beta$ -sheets along with coil, turn and bend, which are consist of the intramolecular hydrogen bonds [9]. In  $\alpha$ -helix the linear amino acids are converted into right hand spiral conformation i.e. the helix conformation. The amino acids in  $\alpha$ -helix are arranged in right handed helical structure in which  $\alpha$ -helix have 3.4 residues per turn and pitch of 5.4 Å. The average length for  $\alpha$ - helices is approximately 12 residues for three helical turns and length is approximately 18 Å. To avoid the steric hindrance the side chains of amino acids design outward and downward from the helix. The chain of amino acids in  $\alpha$ -helix is tightly packed by Vander Waals interactions. When linear chains of amino acids convert into sheets is called  $\beta$ -sheets. Unlike  $\alpha$ -helix the  $\beta$ -sheet forms extensive intramolecular hydrogen bonding. But these are not a stable structure of proteins because they are empathic in nature, i.e. they show both hydrophobic as well as hydrophilic properties (**Figure 3**) [10].

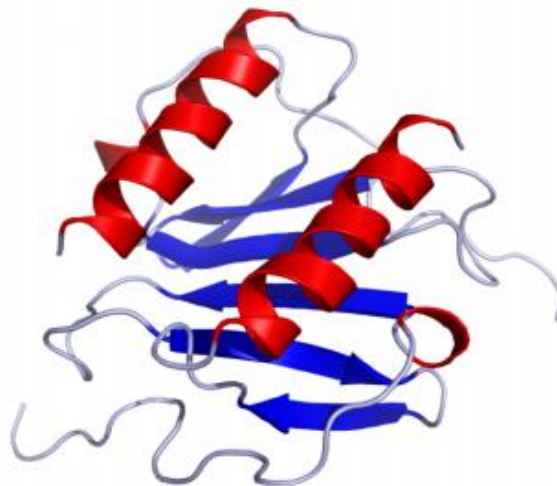


**Figure 1.3:** Ribbon diagram showing the solution structure of human interleukin8. The red spirals indicate  $\alpha$ -helices while the blue arrows show  $\beta$ -sheets. Both of these structures are components of a protein's secondary structure.

**1.2.3 Tertiary structure:** Tertiary structures are a 3-dimensional and functional form of proteins and contain different secondary structure components. In the tertiary structure of proteins polar side chains facing aqueous environment and non-polar side chains facing hydrophobic part of protein. The structures are stabilized by hydrophobic interaction and disulphide bonds between cystein residues [11].

### 1.3 Alzheimer's diseases:

AD is a neurodegenerative, irreversible and progressive diseases. It is the most common cause of dementia affecting over 40 million people worldwide, but still there is no proper cure for this disease till now. According to World Alzheimer's report 2018 the rate of AD enhanced by three times approximately by 2050. AD is the 6<sup>th</sup> major cause of death in the united state. According to report approximately 5.7 million people in America suffers with Alzheimer's in 2018 (**Figure 4**). This includes 5.5 million people of age 65 and above and approximately 200,000 below age of 65 and two-third of Americans suffers with Alzheimer's are women. In every 65 seconds in united state someone develop AD and by mid of century in every 33 seconds someone will develop with AD in the United States. According to official records death from AD increased day by day. As per record, death between 2000 and 2015 increased by 123 percent whereas death from heart disease decreased by 11 percent. In 2018 American society cost \$277 billion for AD and by estimation, in 2050 it crosses \$ 1.1 trillion. Several years after find of AD the mechanism of development is not yet fully understood, its cause depends on many factors like genetic, environmental as with neurodegenerative factors. The two greatest risk factors for AD are age and genetics. But with the progress of AD, the rate of drug research has increased noticeably over the last decades. At present, Familial Alzheimer's disease (FAD) has been approved four drugs for AD. These drugs, however, are not able to prevent the progression of disease [12].

## Projected Number of People Aged 65 or Older With Alzheimer's Disease, by Age Group, United States, 2010-2050

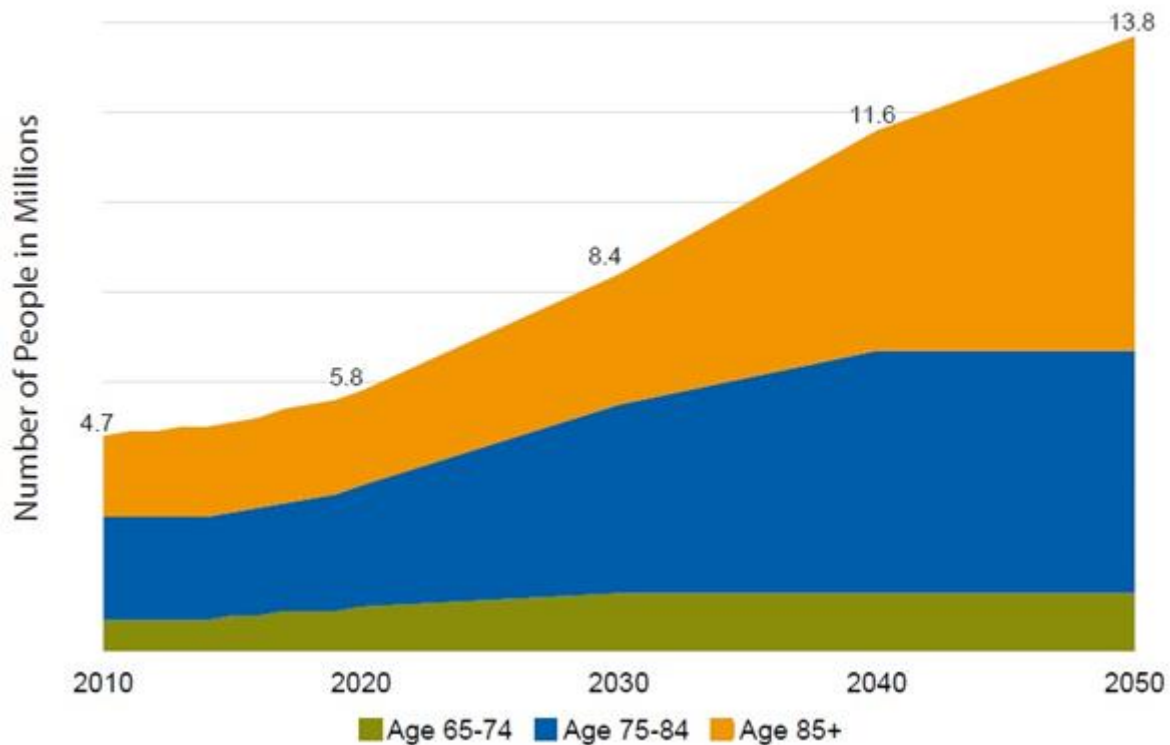


**Figure 1.4:** united states 2010-2050 dementia statistics.

### 1.4 Causes of Alzheimer's diseases

According to the “amyloid cascade hypothesis” the generation of  $A\beta$  would happen from the amyloid precursor protein (APP), and it would aggregate in extracellular insoluble plaques [13]. One of the major characteristics and chronic marks of AD is shown by the senile plaques and neurofibrillary tangles. Now days, protein misfolding is known as beta amyloid plaques and neurofibrillary tangles. These plaques and tangles affect the activity of brain or kills brain cells. APP is present in cell membranes of all neurons [14]. There are three types of enzymes  $\alpha$ -secretase,  $\beta$ -secretase,  $\gamma$ -secretase which are responsible for cleaving or cleavage of  $A\beta$  from APP. Normally protein is cleaved by  $\alpha$  and  $\gamma$  secretase but in case of AD protein is proteolytically cleavage by  $\beta$  and  $\gamma$ -secretase.  $\beta$ -secretase cleaved the protein and created a fragments which are non-soluble and have a tendency to aggregate together (Figure 5). The  $A\beta$  aggregation of insoluble things forms plaques. The  $A\beta$  aggregation blocks cell to cell signaling and transmission between cells, which also seems to activate the immune reaction that causes irreparable damage nerve cells [15].

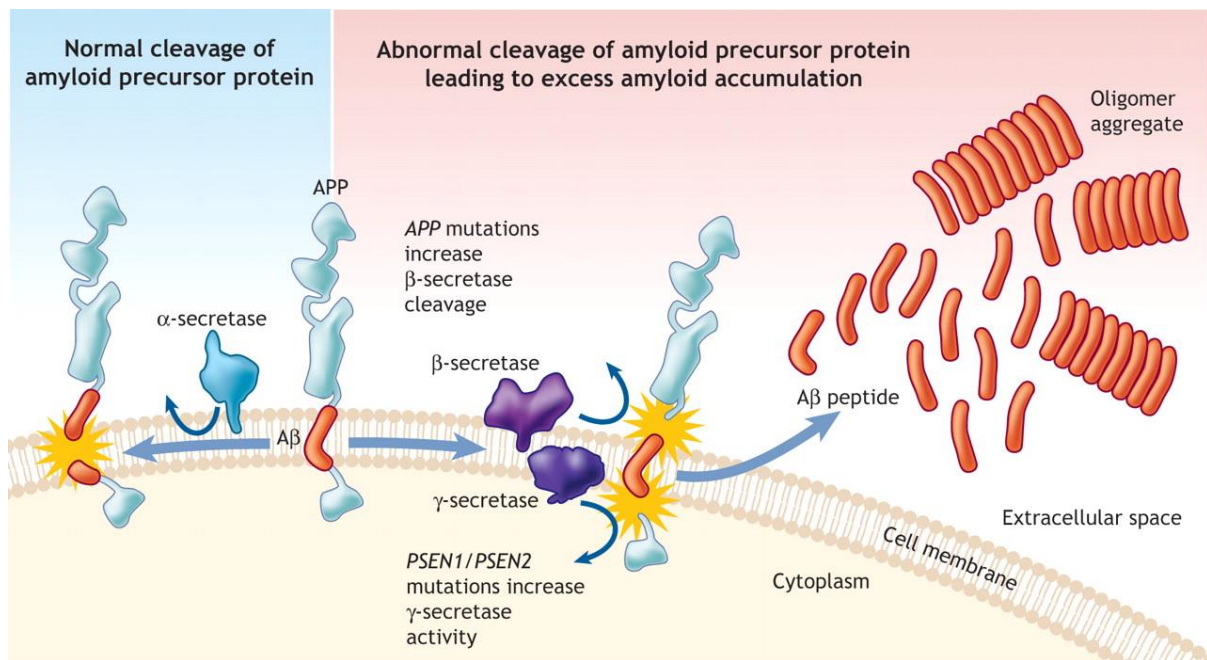


**Figure 1.5:** cleavage of beta amyloid precursor proteins.

In AD, neurofibrillary tangles are built from protein known as tau. Neurofibrillary tangles are formed by hyperphosphorylation of a microtubule. The brain nerve cell contains a network of tubes that act like a highway for food molecules [16]. But in AD, the protein collapses into twisted strands or tangles, making the tube disintegrate, stop nutrients from reaching the nerve cell and leading to cell death. The process that obliteration starts in a region called hippocampus, which is responsible for making memories [17]. Therefore, short term memory loss is the first symptoms of AD. Next, they affect the region that control emotions, resulting in mood swings. At the top of the brain they cause monomania and hallucination and once they reach the brain's rear, the plaques and tangles work together to erase the mind deepest memories. Eventually the control centers governing heart rate and breathing are overpowered as well as resulting in death. The extremely devastating nature of the disease has thrilled many researchers to look for relief, but presently they are targeted at slowing its development [18]. One short term treatment helps lessen the breakdown of acetylcholine, an important chemical messenger in the brain, which is decreased in Alzheimer's patients owing to the permanent end of nerve cell that make it another possible solution is a vaccine that trains the body immune system to attack A $\beta$  plaques before they can form a cluster[19].

### 1.5 Beta-site amyloid precursor protein cleaving enzyme 1 (BACE-1)

BACE-1 is a member of aspartyl protease and also called memapsin-2[20]. BACE is an important target for the development of anti-Alzheimer's agents. BACE-1 breaks APP into N-

terminal give sAPP $\beta$  and C-terminal fragments called C99. A large fragment sAPP $\beta$  is allowed to leave from the cells whereas C99 remains in the cell membrane and is then organized by  $\gamma$ -secretase to produce A $\beta$  peptides (A $\beta$ 40 and A $\beta$ 42)[21]. The enzyme not only cleaves protein, but also neuregulin and  $\beta$ 2 subunit of voltage-gated sodium channel, which play an important role in the functions of the brain. A $\beta$  aggregates resulted to form toxic oligomers and overproduction of A $\beta$  damages the nerve cells of the brain and result to AD [22].

The first report of BACE-1 gene was observed in mice, which reveal that the animals developed normally. Furthermore, studies marked in mice synaptic plasticity and myelination decreased and also shows a loss in cognition and emotion performance test. Although, BACE-1 have been proven to control progress of A $\beta$  in the brain of mice. Therefore, after the discovery of BACE-1 inhibitors both academia and pharmaceutical companies look BACE-1 as potential therapeutics to stop the progress of AD [23].

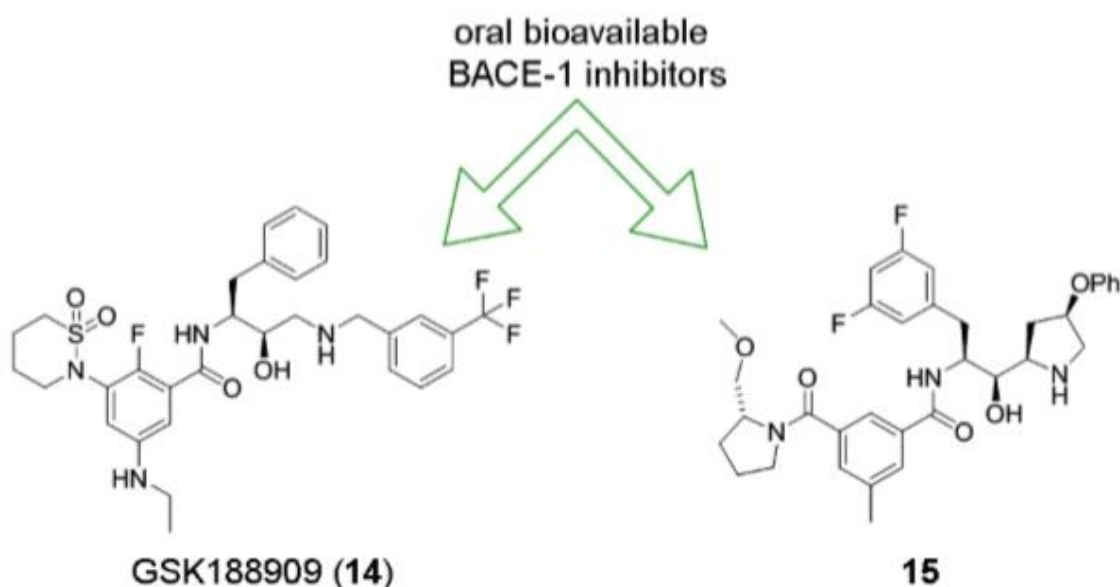


**Figure 1.6:** Chemical structure of first oral bioavailable BACE-1 inhibitors.

In 2007, according to GSK reported the first orally available BACE-1 inhibitor GSK188909 (14), a small non-peptide compound initiated from substrate-based design (Figure 6). GSK188909 (14) displayed a cellular IC<sub>50</sub> of 5 nM and showed excellent selectivity over other aspartic proteases. When orally administered in TASTPM mice, an *in vivo* model which expresses both mutant APPSWE and PS1 mutant (Met146  $\rightarrow$  Val), GSK188909 (14) effectively reduced brain A $\beta$  levels. Subsequently, Schering-Plough also reported an orally effective 4-phenoxy-pyrrolidine-based BACE-1 inhibitor, 15, (Figure 6), with good pharmacokinetics and selectivity (K<sub>i</sub> = 0.7 nM, cellular IC<sub>50</sub> = 21 nM).

In 2008, CoMentis has developed the BACE-1 inhibitor CTS-21166 have IC<sub>50</sub> of 1.2-3.6 NM. Its result satisfied up to Phase II clinical trial. CoMentis make a small compound as a transition state analogy inhibitor having excellent properties in selectivity, metabolic stability and oral availability. When IP injected (4mg/kg over six weeks) into an aggressive APP transgenic mouse, CTS-21166 reduced the A $\beta$  level in the brain by over 35% and plaques by 40%. The Phase I clinical trial suggested that this compound appeared safe as 225 mg and when it's injected into AD patients, it reduces levels of A $\beta$ . Wyeth reported compound WY-25105 (16) of IC<sub>50</sub> - 3.7 $\mu$ m, cellular IC<sub>50</sub> - 20 $\mu$ m form interaction with Asp32 and Asp 228. Furthermore this compound led to the occurrence of more potent BACE-1 inhibitors 17 with IC<sub>50</sub> of 0.11 $\mu$ m. Using the same criteria, Johnson and Johnson developed the BACE-1 inhibitor 18 having a stronger interaction for BACE-1 ( $k_i$  - 11nm) and results in excellent brain permeability and oral availability. In fact, when orally administered at 30 mg/kg to rats, 18 was able to decrease the levels, plasma A $\beta$ 40 by 40–70% 3 h post-dosing. Regardless of all of these successes, none of these HTS-based inhibitors have entered a clinical trial [24]. A variety of biophysical techniques like NMR, X-ray crystallography, fluorescence resonance energy transfer (FRET) or surface Plasmon resonance (SPR) computational tools and biochemical assays can be connect in fragment screening[25].

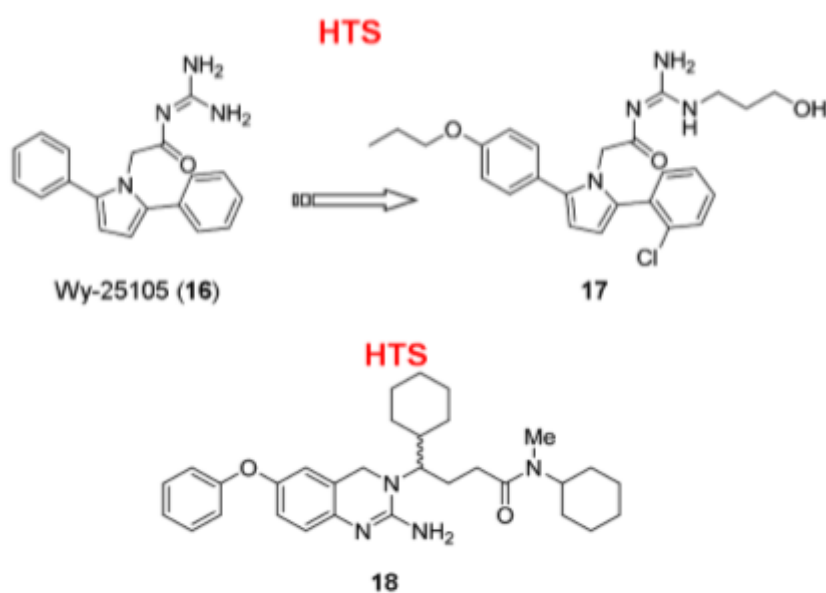


**Figure 1.7:** chemical structure of the non - substrate based BACE-1 inhibitors.

The BACE-1 inhibitors PF-06751979 (64) have broad selectivity (~ 5.6-fold), weak hERG inhibition, stability in plasma and excellent brain penetration over aspartyl protease including

BACE-2. For mouse studies used sensitive immunoassays to measure A $\beta$ 42 in brain homogenates, as well as A $\beta$ 40 in CSF. Acutely, with 50mg/kg, lowering of brain A $\beta$ 42 persisted in dose and time dependent manner with a maximum inhibition of 56%, peaking at 5 to 7 h post dose. Molecule 64 yielded a dose responsive and a time dependent reduction of CSF A $\beta$ 40 with peak inhibition at 3 h of > 77%. Therefore, the safety and tolerability data from longer duration clinical trials with the current BACE-1 inhibitors will establish the impact of chronic inhibition of BACE-2. Compound 64 recently phase 1 clinical trials and reveals potent and dose- dependent A $\beta$  lowering in human CSF [26].

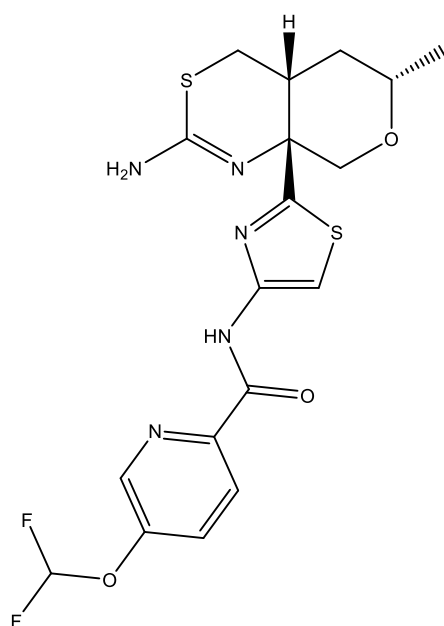


**Figure 1.8:** BACE-1 inhibitor PF-06751979 (64).

BACE1 belongs to the pepsin family under the aspartic protease super family and has the most sequence identity with BACE2 (52%). Catalytic cleft is an important target for the inhibitors to hinder the activity of BACE1. The high conservation of the catalytic cleft among aspartic proteases makes the task of achieving BACE1 selectivity difficult. The majority of BACE1 inhibitors possess tight hydrogen bonding network with the catalytic aspartic residues (Asp32 and Asp228) and other less common residues as well as hydrophobic interactions with the amino acid residues present in the pockets that form the catalytic cleft. O'Neill reported the inhibitor **64** with high selectivity for BACE1 which is further selected to get insight in the present using computations techniques. The computational techniques provide an alternative approach in determining the protein–ligand interactions at an atomic level, which, otherwise, are difficult to elucidate using experimental techniques (Awasthi, Singh, Pandey, & Dwivedi, 2017; Balogh et al., 2017; Bruce, Ganotra, Kokh, Sadiq, & Wade,

2018; Narang, Shuaib, &Goyal, 2017; Zeng & Wu, 2016;Saini, Shuaib &Goyal, 2018; Zhenget al., 2018; Shuaib & Goyal, 2017

Percent identity of the target sequences was calculated with BACE1 sequence (accession code P56817) from NCBI using sequence database search program BLASTP (version 2.2.27) against the non redundant protein sequences database with keyword organism=Homo sapiens (taxid:9606) on Jan 27, 2013 ([http://blast.ncbi.nlm.nih.gov/Blast.cgi?PAGE=Proteins&PROGRAM=blastp&BLAST\\_PROGRAMS=blastp&QUERY=P56817.2&LINK\\_LOC=protein&PAGE\\_TYPE=Blast Search](http://blast.ncbi.nlm.nih.gov/Blast.cgi?PAGE=Proteins&PROGRAM=blastp&BLAST_PROGRAMS=blastp&QUERY=P56817.2&LINK_LOC=protein&PAGE_TYPE=Blast%20Search))

## CHAPTER 2

### 2. Computational details

#### 2.1 System preparation: BACE-1 and protofibril structure

In the present study, four MD simulations were performed in the explicit solvent for 30 ns each. The first system consists of apo-BACE1 which is taken from (PDB ID: 1FKN) [Hong et al., 2002] and the second system consist of a docked complex of **C1** with BACE1. The two systems are named as apo-BACE1 and BACE1-C1 complex.

#### 2.2 Parameterization of C1

The 2D structure of **C1** was drawn using Chem Draw ultra package (**Fig. 1a**) [29]. The **structure** of **C1** was optimized at the HF level of theory with 6-31G basis set using Gaussian 09 [30]. For molecular dynamics simulation, GROMOS96 force field parameters for **C1** were generated using Automated Topology Builder (ATB) [31]. The consistency and effectiveness of ATB parameters are justified by Malde and co-workers; [Error! Bookmark not defined.]. The parameters and charges generated by the ATB server are reliable and widely used in a number of studies (Dalal et al., 2017; dos Santos et al., 2015; Narang et al., 2018; Plazinski et al., 2016; Shuaib and Goyal, 2017).

#### 2.3 Molecular docking

The molecular docking of **C1** with BACE1 was performed using AutoDock 4.2 [32]. For docking between BACE1 and **C1**, grid spacing was kept default (0.375 Å), and the grid dimensions were set to 106 Å × 102 Å × 100 Å with grid center defined at x = 10.772, y = 2.783 and z = 4.617. The population of 100 individuals was used to generate 50 conformations for 27,000 generations with 25, 00,000 energy evaluations. The mutation rate of 0.02, crossover rate of 0.80 and reference RMSD were kept as default. Among the stochastic search algorithms available in AutoDock suite, Lamarckian Genetic Algorithm (LGA) which utilizes global search (Genetic Algorithm) and local search (Solis and Wets algorithm) was chosen for this study.

The docked conformations were clustered using a root-mean-square deviation (RMSD) of 0.20 and the conformational clusters were ranked in order of increasing binding energy. The ligand-receptor interactions were visualized with AutoDock Tools (ADT) and PyMOL [34].

## 2.4 Molecular dynamics simulation and analysis

MD simulations of the model systems were performed using GROMACS (version 5.0.5) with GROMOS96 54a7 force fields [35]. The GROMOS force field has been widely used for the analysis of the conformational changes in peptides in a number of recent studies [36]. The protonation state of BACE1 was assigned to mimic the experimental pH 4.5 using/with the help of pKa values. Protonation state of residues (Lys, Arg, His, Asp, and Glu) was assigned according to their Pka values using PROPKA servers, while N-terminus ( $\text{NH}_3^+$ ) was protonated and C-terminus ( $\text{COO}^-$ ) were deprotonated for the simulation (Li et al., 2005; Søndergaard et al., 2011). The docked complex was immersed in the cubic box and the minimum distance from the complex to the edge of box for apo-BACE1 was kept 1.1 nm with a box size of 9.2 nm  $\times$  9.2 nm  $\times$  9.2 nm. The box was solvated with simple point charge (SPC) water model [37], and the protein-water system was subjected to energy minimization. The time step was set to 2 fs, using LINCS method to constrain the bond lengths and Berendsen coupling algorithm was applied to keep the temperature and pressure constant. The cut off value of short-range Vander Waals interactions was kept 1.0 NM and long-range electrostatic interactions were calculated using the particle mesh Ewald (PME) method [39]. The system was equilibrated under NVT conditions for 100 ps at 300 K followed by 100 ps under NPT conditions. MD simulation for each system was performed for 200 ns under periodic boundary conditions and the trajectories were saved at 10 ps interval.

The analysis of the MD trajectories was performed using GROMACS. The MD trajectories were analyzed using visual molecular dynamics (VMD) [40] and the graphics were generated using PyMOL [Error! Bookmark not defined.] and Origin (version 9.5). The GROMACS utility gmx cluster tool was used for the conformational clustering. The chosen cut off for the conformational clustering ensures that the root-mean-square deviation (RMSD) of any two snapshots included in a single cluster was less than 0.20 nm. The global structural changes were analyzed using RMSD and RMSF. The compactness of A $\beta$ <sub>42</sub> monomer and protofibril was assessed using the gmx gyrate tool. The GROMACS utility gmxmindist and gmx distance was used to the hydrogen bond distance between BACE1 residues and C1. The GROMACS utility gmx h-bond was employed to calculate the number of backbone hydrogen bonds.

## CHAPTER-3

### Literature Review

In 2010 Hu *et al.*, Have designed and synthesized 1, 3-diphenylurea derivatives as dual-target-directed agents by undergoing hybridization of the metal chelators LR-90 with BACE1 inhibitor. Designed structures of 1, 3 diphenylurea derivatives were tested and analyzed with the primarily formed BACE1 inhibitor pharmacophore model[41].

Hamley *et al.*, studied about biological and biophysical properties of A $\beta$  peptide and its role in AD. The biological, neurochemical and biochemical attributes of AD had been discussed which also involve A $\beta$  and APP. Treatment to limiting the pace of disease had been discussed including those along the market and subject of clinical tests. Number of compounds is available to control the former level of AD. Coming up a selective therapeutic agent is challenging given the form of biochemical pathways involved in brain signaling and other neuronal growth and differentiation process. With aspects of biophysical chemistry, it bears to be noted that control of A $\beta$  aggregation is difficult due to highly sensitive to sequence, purity and preparation condition. Further factors include initial dispersal solvent, the nature and concentration of the aqueous or buffer solution. Despite all these data on fibrilization properties of A $\beta$ , variants and fragments under a defined condition which help in biological research activity[42].

In 2014 Barman *et al.*, reported the application of computational methodologies provide information regarding substrate, site specificities, catalytic mechanism and protonation state of the catalytic Aspartic dyad of BACE-1. Molecular dynamic (MD) simulations help to understand the difference in the structure of enzymes, responsible for observed differences in structural activities toward the WT and SW-substrate. Experimental observation tells perfection of the structural information regarding the enzyme-substrate interaction requires additional advancements. In substrate-protein interaction, the catalytic mechanism can be improved by hydrophobic interaction. Quantum mechanical (QM) calculation indicated that BACE-1 hydrolyzed the SW-substrate more effectually than the WT - substrate. The effects of molecular docking showed that the data regarding a single protonation state of Aspartic dyad is not plenty to run a silico screening campaign[43].

In 2014, oral active drug BI1181181 show strong potency in reducing brain A $\beta$  aggregation in phase 1 clinical trials but this compound not cleared the clinical trials in 2015 so Boehringer has closed development of BI1181181 due to side effects of this experimental BACE-1 inhibitor drug. From all result, it should be recognized that BACE-1 is best target to reducing A $\beta$  aggregation but still require to find new molecules to inhibit the activity of BACE-1

In 2015, XiaomingZha et al. reported twenty-six hybrids out of which 2e hybrid compound showed good inhibition of hAChE and of both A $\beta$  aggregation and hBACE-1 activity. Kinetics studies showed that 2e acted as a slow, tight-binding, mixed-type inhibitor, while X-ray crystallographic studies highlighted the ability of 2e to induce large-scale structural changes in the active site gorge of Torpedo Californica AchE [44].

In 2016, Yan *et al.*, summarized various strategies that successfully led to discovery of BACE-1 drugs such as MK8931, AZD-3293, JNJ-54861911, E2609 and CNP520. Drugs LY-2811376 and LY-2886721 were terminated; cause side effects due to evidence of liver toxicity in patients [46].

In 2016 Scott *et al.*, Verubecestat 3(MK-8931) is high affinity BACE-1 inhibitors, cleared phase 2 clinical trials for the treatment of AD. Verubecestat 3 show more selectivity for BACE-1 over BACE-2. Compound 3, BACE-1 inhibitors with suitable CNS drugs like properties. Compound 3 structural features provide strong central pharmacodynamics activity and lower the unenviable off-target activities. Efflux susceptibility and permeability of compound 3 by reduced basicity of iminothiadiazinane dioxide and by the existence of an intramolecular hydrogen bond between amide hydrogen and amide. High BACE-1 affinity underscored the importance of N-phenylpicolinamide S1 – S3 binding sites. Verubecestat 3, BACE-1 inhibitors that has approached to phase 3 clinical trials for AD. Further study revealed that a phase 3 clinical trial has failed because of which compound 3 not used for treatment of AD in humans[47].

In 2016, Timmers *et al.*, concluded that JNJ-54861911 could bind to BACE-1 and used as potential drug to design B ACE-1 inhibitors for AD therapy[48].

In 2017, Shuaib *et al.*, performed molecular dynamics study to investigate the inhibitory mechanism of Dicyanovinyl substituted J147 derivative against A $\beta$ 42 oligomers formation and fibril disassembly. The authors concluded that the inhibitor stabilized the A $\beta$ 42 monomer in its' native conformation and destabilized the A $\beta$ 42 protofibril. In this regard we plan to find the inhibitory mechanism of small molecules against A $\beta$  aggregation and BACE-1 activity using molecular dynamics tools[49].

In 2017, Kumar *et al.*, performed screening of approximately 150 antipsychotic drugs on five major target (AChE, BuchE, BACE-1, MAO, and NMDA) by molecular docking. Favourable drug compared with formerly known inhibitor of specific proteins. Antipsychotic drugs such as anisoperidone, benperidol, pimozide, bromperidol, melperone and anisopirol showed better docking score and binding energies to the known inhibitors of the specific targets. Benperidol was found the best drug interacting with different target protein involved in AD[51].

In 2017, Ruderisch *et al.*, designed BACE-1 inhibitors with changing lipid modification with single-digit picomolar cellular potency. Secondly, generated active- exist peptides with structurally chronic dual binding mode and good potency. When fused to the brain shuttle (BS), these BACE-1 inhibitors reduced A $\beta$  in the brain of mice after intravenous administration and conclude that BS is necessary for BACE-1 peptide inhibitors to the effect in the brain and active-exquisite design of the BACE-1 inhibitors with lipid modification may be therapeutically important[52].

In 2018, Kumar *et al.*, performed molecular docking, Molecular dynamics (MD) and binding energy (MM-PBSA) study to investigate the naphthofuran derivatives. During docking (NS7 and NS9) showed a better binding affinity. Selectivity of BACE-1 inhibition occurs due to the formation of good interactions with the flap residues Gln73, Thr72 and Arg 141, Thr 138 residue of GSK-3 $\beta$ . The outcome suggested that naphthofuran derivatives may act as dual inhibitors against BACE-1 and GSK-3 $\beta$ [53].

In 2018, Thai *et al.*, concluded that CID9998128 could bind to BACE-1 due to Vander Waals interaction and used as a potential lead drug to design a novel BACE-1 inhibitor for AD therapy[54].

## CHAPTER-4

### 4. Results and discussion

#### 4.1 Binding region analysis using docking analysis

O'Neill et al., shortlisted **64** (**C1**) which significantly shows good brain penetration and high selectivity over BACE1 active site. In the present study molecular docking and MD simulations were performed to get across the mechanism and key interactions of **C1** responsible for its *in vitro* inhibitory activity against BACE1. **C1** is a thiazole-amides based compound (**Figure 4.1b**) designed by modifying pKa by including the fluoro group and increased exposure in brain. Author reported that **C1** appear as best clinical candidate with great potency and also shows good selectivity for BACE1. The electrostatic interactions of the compound with catalytic aspartic residues (Asp32 and Asp228) is essential for a compound to act as an BACE1 inhibitor as well as hydrophobic interactions with the residues present in the pockets that form the catalytic cleft .

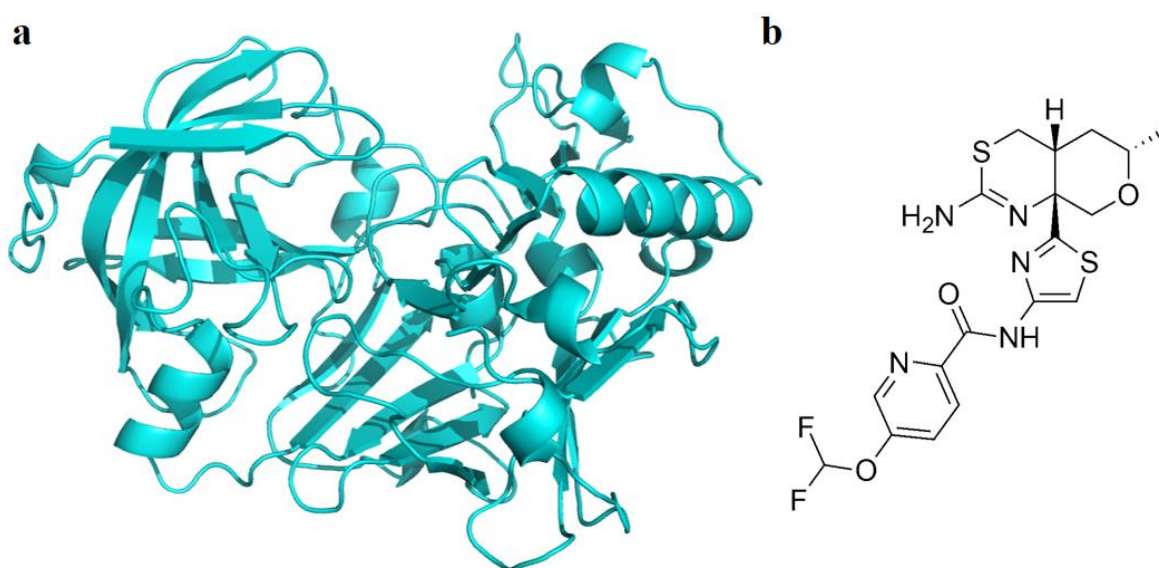


**Figure 4.1.** Cartoon representation of BACE1 enzyme (PDB ID: 1FKN) is shown in panel a. The 2D chemical structure of PF-06751979 (**64** or **C1**) ligand is shown in panel b.

The docking analysis was performed to predict/understand the favored binding modes and key interactions of **C1** responsible for the inhibition of BACE1 activity. The docking results show/represent that the binding energy of **C1** with BACE1 is  $-5.9$  kcal/Mol. The interactions in the best docked pose of BACE1-**C1** complex confirms the presence of one hydrogen bond (**Figure 4.2b**). The nitrogen atom of pyridine moiety participates in hydrogen bond formation with Arg235 residues of BACE1. The **C1** also shows the hydrophobic contacts with different

active catalytic pocket residues i.e. S1 (Tyr71 and Phe108), S1' (Tyr71 and Thr72), S2 (Arg235), S3 (Ile110) and S4 (Gln73 and Thr232) of BACE1 (**Figure. 2b, c Table 1**). The terminal rings of **C1** take part in hydrophobic interactions with Tyr71, Thr72, Gln73, Lys107, Phe108, Ile110, Gly230, Thr231, Thr232 and Arg235 residues of BACE1 as shown in (**Figure 4.2b**).(Table 4.1).

**Table 4.1.** Molecular docking analysis of BACE-1 and C1 using Autodock.

AutoDock binding energy (kcal/mol)	Residues participating in intermolecular hydrogen bonds with C1			Residues involved in hydrophobic contacts with C1
	Residue	Atoms <sup>a</sup>	Distance (nm)	
-5.9	Arg235	1NH1 : N	0.22	Tyr71, Thr72, Gln73, Lys107, Phe108, Ile110, Gly230, Thr231, Thr232, Arg235

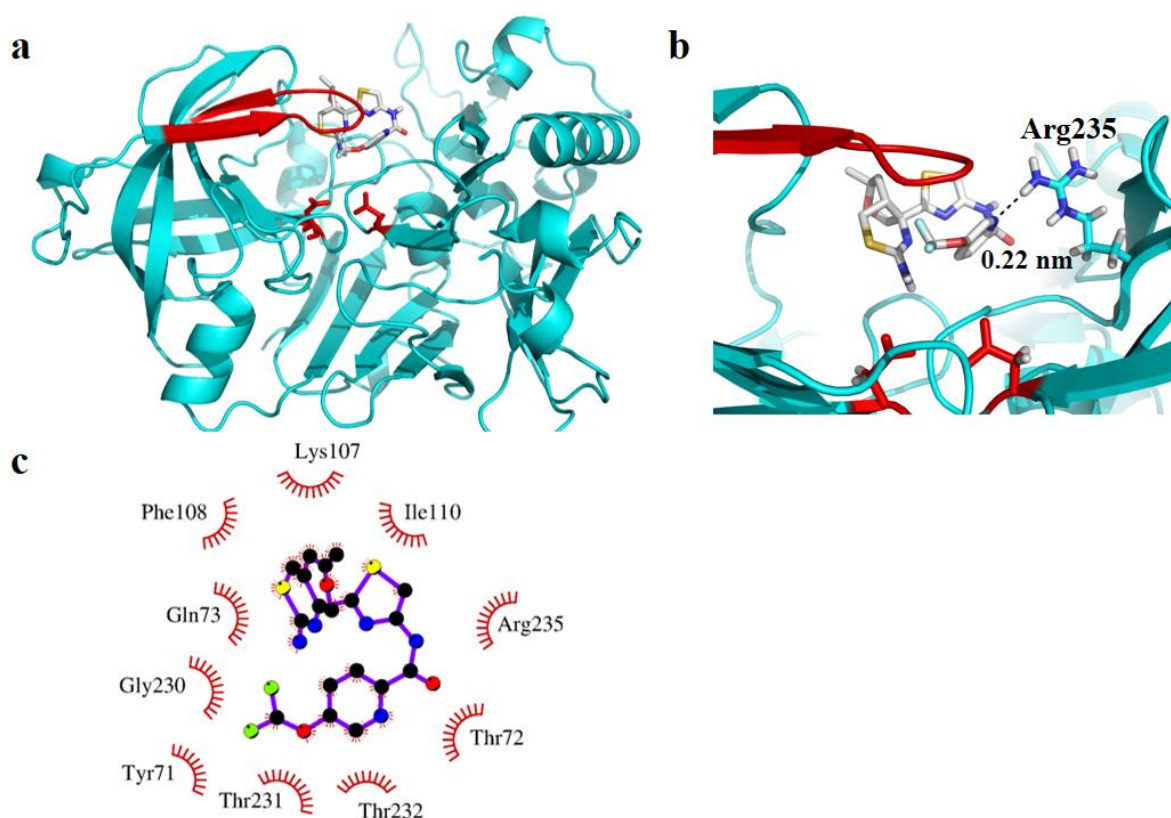


**Figure 4.2.** The best docked complex of BACE1 with **C1** is shown in panel a & b. BACE1 is shown in the cartoon representation and ligand is shown in the stick representation. The 2D interaction maps of hydrophobic contacts of BACE1 residues are shown in red semicircles with C1 as shown in panel c. The 2D maps were generated using LigPlot+ software.

The observed inhibitory activity of **C1** is shown due to the interactions with key active pocket residues along with flap residues. The MD simulations were performed to further investigate the inhibitory activity of **C1** against BACE1.

## 4.2 Results of molecular dynamics simulations

MD simulations have been extensively employed to complement experiments in studying the detailed information on the structure of various A $\beta$  forms in aqueous environment as well as in the elucidation of the inhibitory mechanism of various inhibitors against A $\beta$  aggregation (Azam et al., 2017; Nasica-Labouze et al., 2015; Saini, Shuaib, Goyal, & Goyal, 2017; Shea & Urbanc, 2012; Shuaib & Goyal, 2018). In present study MD simulations were performed at acidic pH (4.5) using GROMOS 54a7 force field.

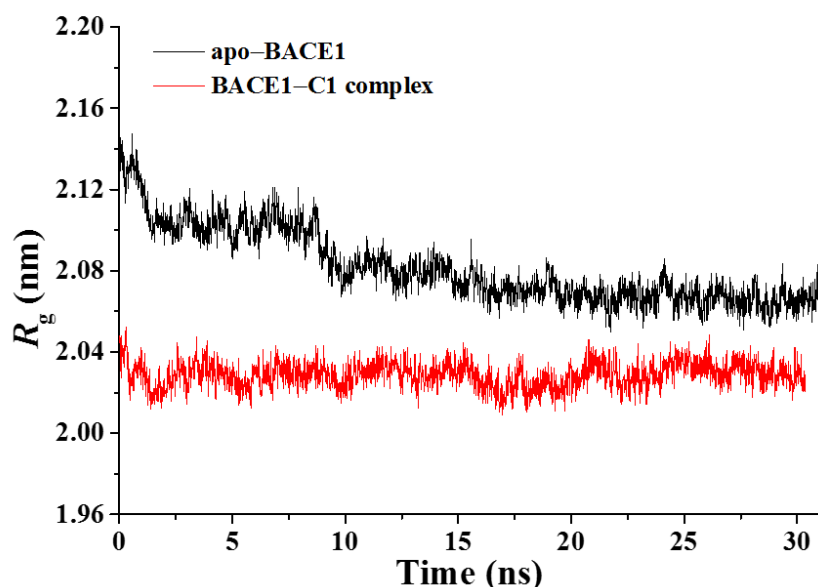


**Figure 4.3.** The radius-of-gyration ( $R_g$ ) of apo-BACE1 (black) and BACE1-C1 complex (red) during simulation.

The conformational ensembles were evaluated using RMSD,  $R_g$  and RMSF for both apo-BACE1 and BACE1-C1 complex. The results of apo-BACE1 indicate fluctuations decreases in  $R_g$  during the simulation time. After that,  $R_g$  remain stable at an average 2.08 nm for apo-BACE1 as shown in figure. Whereas BACE1-C1 complex shows fluctuations to relatively lower values as observed for apo-BACE1 and average of  $R_g$  was calculated to be 2.02 nm for BACE1-BTT complex, which shows overall structural stability of BACE1 in both systems (Figure 3).

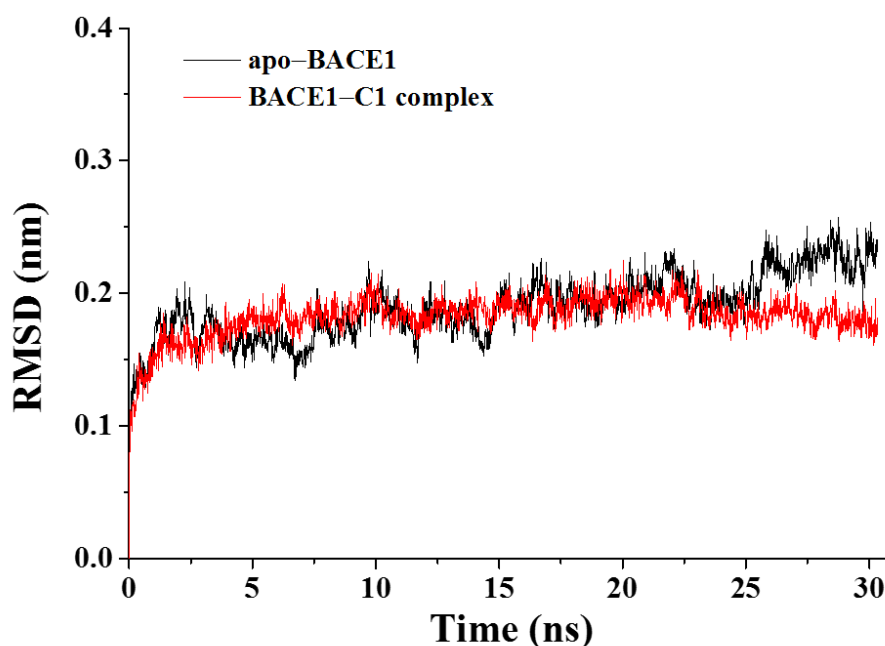


**Figure 4.4.** The root-mean-square deviation (RMSD) of apo-BACE1 (black) and BACE1-C1 complex (red) during simulation.

The stability was also indicated by time dependence of backbone RMSD obtained from MD trajectories. The apo-BACE1 represent higher fluctuations in backbone RMSD till the end of simulation as compare to BACE1-C1 complex as shown in Figure 4. Kumalo and Soliman (2016) reported that RMSD fluctuations within 0.1–0.2 nm represent a stable trajectory for further analysis of apo-BACE1. In the present study, the average backbone RMSD for apo-BACE1 and BACE1-BTT complex is 0.18 nm. The backbone RMSD of BACE1-C1 complex represent similar average value of 0.18 nm but RMSD fluctuate at marginally lower throughout the simulation as compare to apo-BACE1 (Figure 4). The RMSD and Rg results do not demonstrate any structural instability and provide suitable basis for further investigations.

The  $C\alpha$  RMSF was calculated for both the systems which highlight that ~80-85% of residues of BACE1-C1 complex shows fluctuation at lower value as compare to apo-BACE1. The higher  $C\alpha$  RMSF for apo-BACE1 was expected for the flap region (Gly66-Glu77) and loops (insert -A, -C, -D, -F and 10s loop) located near the active site, which is reported in earlier studies (Andreeva and Rumsh, 2001; Kumalo and Soliman, 2016; Patel et al., 2004; Spronk and Carlson, 2011).

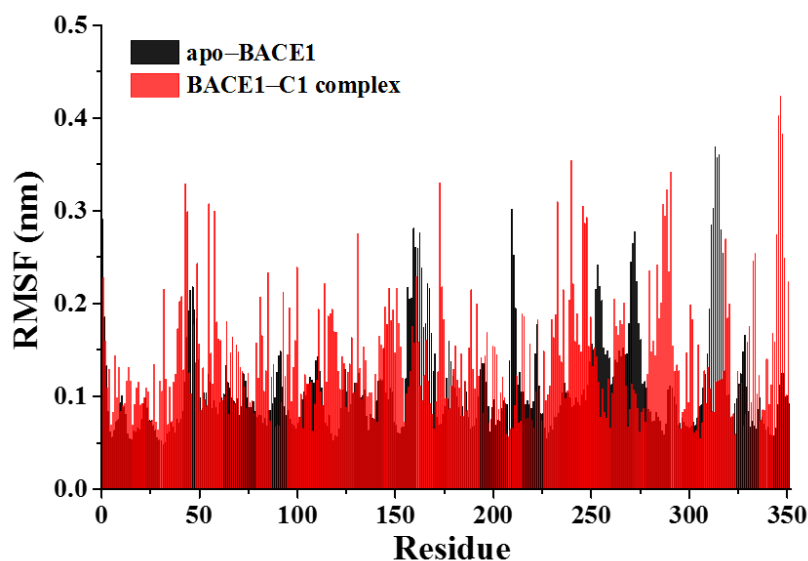


**Figure 4.5.** The  $C\alpha$  root-mean-square fluctuation (RMSF) of each residue for apo-BACE1 and BACE1-C1 complex is shown in panel c.

**C1** shows the significant reduction in the fluctuation of loop regions i.e. insert-A (Phe159-Leu167), insert-B (Lys218-Asn221), insert-C (Ala251-Pro258), insert-D (Trp270-Gly273), insert-E (Glu290-Ser295) and insert-F (Gln316-Asp318) as compare to apo-BACE1 along with 10s loop residues (Lys9-Tyr14) which is also reported to be an important loop (Figure 5). Xiong et al. (2004) suggested that the motions of the inserts-A, D and F change the shape of active site and involve in substrate entry. Fluctuation on flap region (Gly66-Glu77) also decreases as compare to apo-BACE1 which may be due to binding of **C1** with flap residues. The results highlight that binding of **C1** reduce flexibility of insert-A and insert-F in BACE1.

#### 4.2.1 Binding interactions of C1 with BACE1

The hydrogen bond and hydrophobic contacts play critical role in the formation of stable protein-ligand complex. The hydrogen bonds were analyzed between BACE1 and **C1** during simulation time. The average number of hydrogen bonds were calculated  $\sim 2$  (1.8) and range between 0-5 during simulation among BACE1 and **C1** (Figure 6). Further hydrogen bond profile was analyzed from the center member of top most cluster of BACE1-C1 complex. Three residues i.e. Gln73, Thr232 and Asn233 participate in the hydrogen bond formation with **C1** (Figure 6). To get more insight distance was calculated for simulation time with average distance of 0.19 nm, 0.23 nm and 0.19 nm for Gln73, Thr232 and Asn233, respectively (Figure 7).

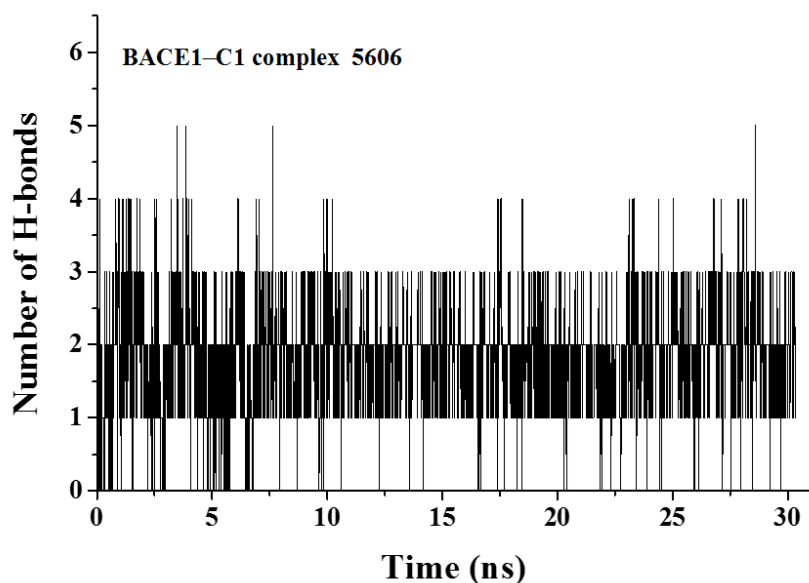


**Figure 4.6.** The number of hydrogen bonds between BACE1 and C1 during simulation with value on the top of the graph indicates the total number of hydrogen bonds.

BACE1 is an enzyme having a large active pockets with hydrophobic residues, therefore hydrophobic contacts are important forces in the development of BACE1 inhibitors (Xiong et al., 2004). The hydrophobic contacts were analyzed using LigPlot+. The BACE1-C1 complex shows that Gly11, Gln12, Thr72, Gln73, Phe108, Ile110, Trp115, Gly230, Thr231, Thr232 and Asn233 residues were participate in hydrophobic contacts with C1 (Figure 7). The residues were projected/present in S1 (Gln73 and Phe108), S1' (Thr72), S2 (Asn233), S3 (Ile110) and S4 (Gln73 and Thr232) active pockets. Similarly, earlier reported inhibitors AZD3839 and HEA derivatives showed the interactions with S1, S1' and S2' active pockets (Jeppsson et al., 2012; Wu et al., 2016).

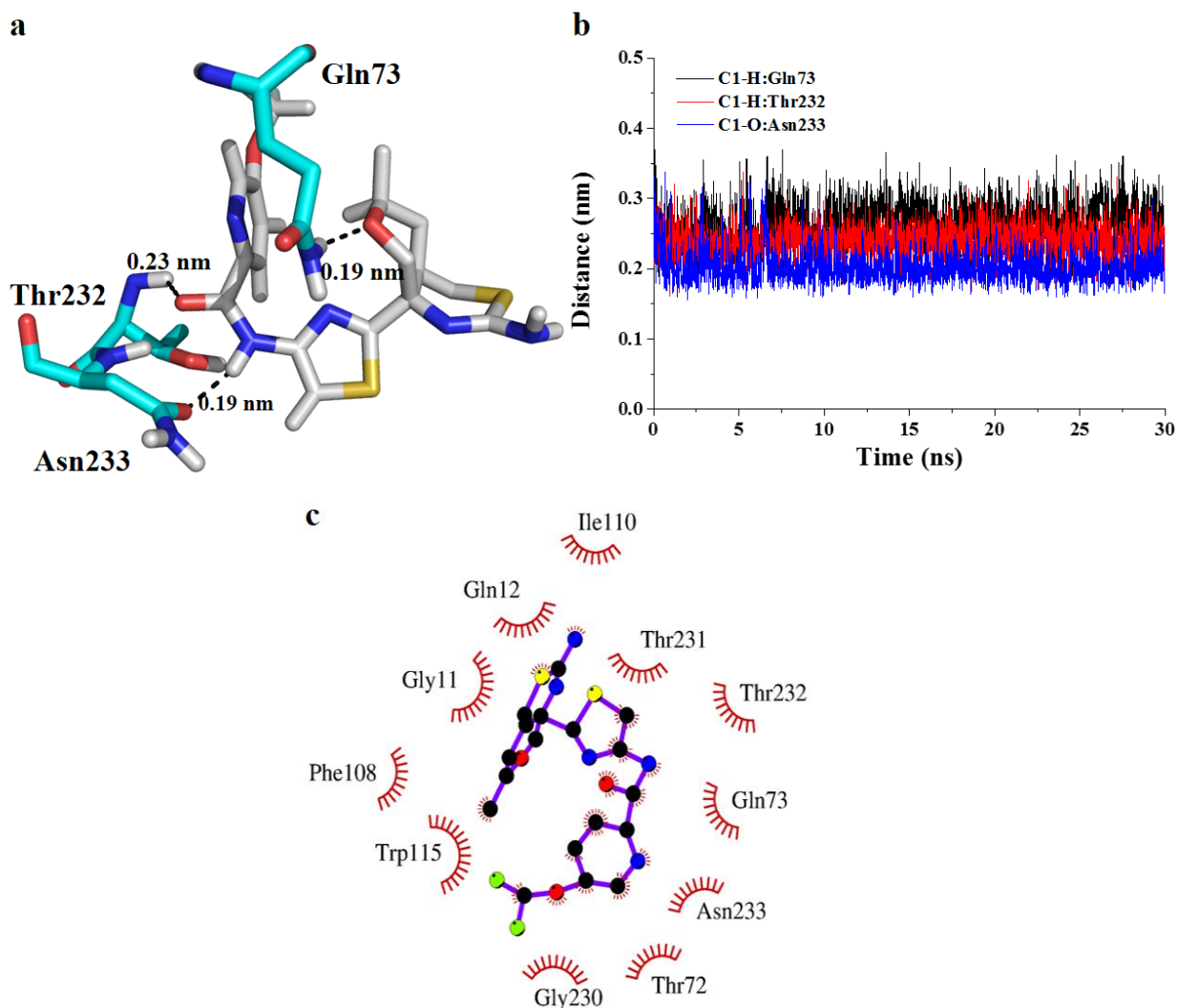


**Figure 4.7.** The snapshot of central member of top most cluster represent hydrogen bond interactions between BACE1 residues and **C1** is shown in panel a. The time dependence of distance between Gln73, Thr232 and Asn233 is shown in panel b. The 2D interaction maps of hydrophobic contacts of top most cluster of BACE1 residues are shown in red semicircles with **C1** as shown in panel c.

#### 4.2.2 Flap confirmation

Flap region is crucial for protease inhibitor design (Hornak et al., 2006) and modification in the position of flap (open and close) play critical role in the activity of BACE1 and propagation of ligand in and out of active site (Hong and Tang, 2004; Shimizu et al., 2008). So it is important to study the movement of flap region. Earlier study reported that interatomic distance range from 1.0 nm to 1.4 nm indicate a close to open flap conformation, respectively (Dhanabalan et al., 2017).

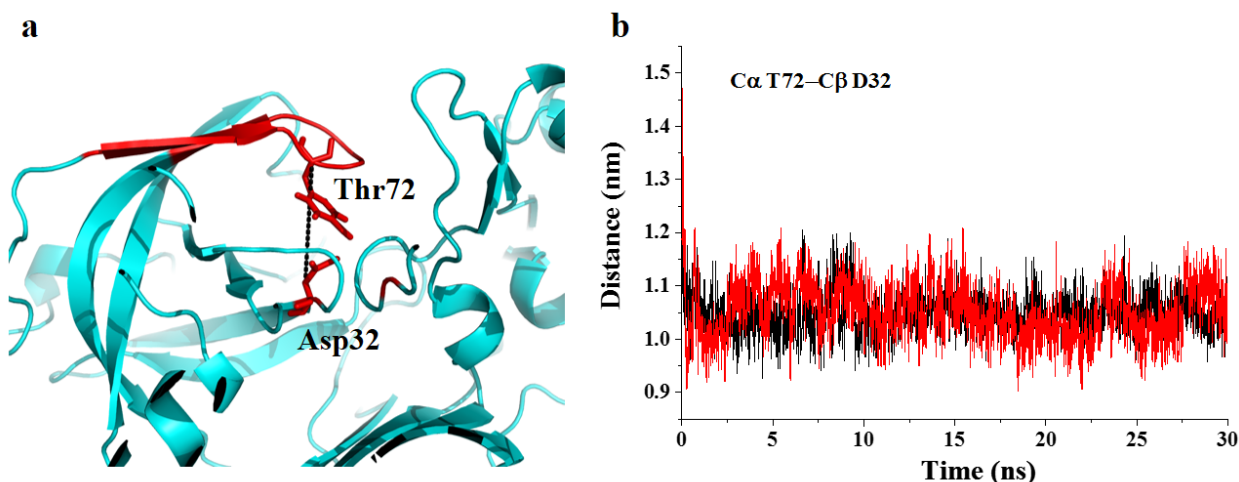


**Figure 4.8.** Snapshot of flap dynamics (panel a) and interatomic distance between C $\alpha$  Thr72 – C $\beta$  Asp32 of flap region for apo-BACE1 (black) and BACE1-C1 complex (red) during the course of simulation time (panel b).

To get more insight into flap movements, the interatomic distance was calculated between C $\alpha$  Thr72 – C $\beta$  Asp32 and C $\alpha$  Tyr71 – C $\beta$  Asp32 atoms for both the systems during simulation time (Barman et al., 2011; Kumar et al., 2016). The distance between C $\alpha$  Thr72–C $\beta$  Asp32 atoms of apo-BACE1 shows average (1.04) with in close distance range (**Figure 4.8**). Whereas in BACE1–C1 complex shows similar average (1.05) and confirms that flap remain in close conformation after inserting C1 in active site as shown in **Figure 4.8**.

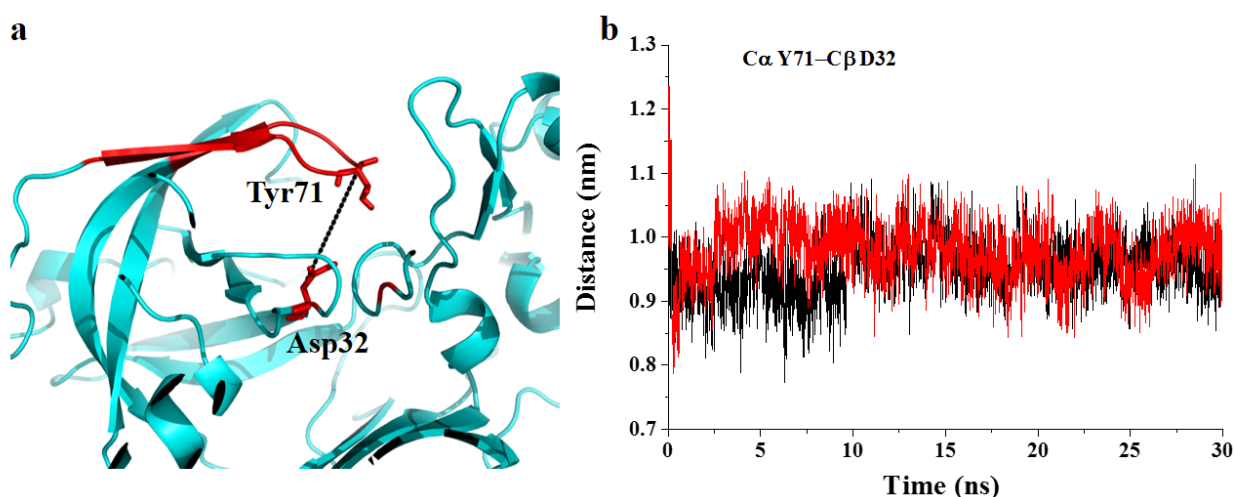


**Figure 4.9.** Snapshot of flap dynamics (panel a) and interatomic distance between C $\alpha$  Tyr71 – C $\beta$  Asp32 of flap region for apo-BACE1 (black) and BACE1-C1 complex (red) during the course of simulation time (panel b).

Earlier studies also reported that Tyr71 as tip of flap region (Hong et al., 2002), therefore interatomic distance between C $\alpha$  Tyr71–C $\beta$  Asp32 is also calculated. Apo-BACE1 exhibit similar fluctuations as in case of BACE1–C1 complex distance and average is come out to be

0.95 nm and 0.97 nm for C $\alpha$  Tyr71–C $\beta$  Asp32, respectively (**Figure 4.9**). The results show that C1 bind strongly with flap residues (Gly66-Glu77) and keep the flap in close confirmation and hinder the BACE1 activity.

## CHAPTER-5

### 5. Conclusion

In the present study, the binding of **C1** with BACE1 was investigated by molecular docking and MD simulations to understand the effect of BACE1 activity. MD simulations highlighted that the **C1** bind with catalytic cleft residues and flap residues. The conformation clustering and flap dynamics analysis highlight that **C1** significantly bind with the catalytic cleft and hinder the formation of A $\beta$ <sub>42</sub>. The molecular docking analysis highlight that **C1** preferentially bind to S1, S1', S2, S3 and S4 active pockets. MD simulations highlighted that **C1** stay in active pocket during the simulation time and also shows interactions with flap residues.

The RMSD and Rg results do not demonstrate any structural instability and provide suitable basis for further investigations. **C1** shows the significant reduction in the fluctuation of loop regions i.e. insert-A (Phe159-Leu167), insert-B (Lys218-Asn221), insert-C (Ala251-Pro258), insert-D (Trp270-Gly273), insert-E (Glu290-Ser295) and insert-F (Gln316-Asp318) as compare to apo-BACE1 along with 10s loop residues (Lys9-Tyr14) which is also reported to be an important loop (Figure 5). Three hydrogen bonds were observed with BACE1 residues Gln73, Thr232 and Asn233 with **C1**. **C1** shows interactions with flap residues Thr72 and Gln73 and keep the flap in close confirmation. The results of present study provide insights into the rational design of potent novel inhibitors against BACE1 activity which certainly interfere with A $\beta$  formation and reduce the A $\beta$  aggregation.

## CHAPTER-6

### Reference

1. Anfinsen, C. B. The Formation and Stabilization of Protein Structure. *Biochem. J.*, **1972**, *128*, 737-749.
2. Anfinsen, C. B. Principle that Govern the Folding of Protein Chain. *Science*, **1973**, *181*, 223-230.
3. Dill, K.A. Theory for the Folding and Stability of Globular protein. *Biochemistry.* , **1985**, *24*, 1501-1509.
4. Clark, P.L. Protein folding in the cells: Reshaping the Folding Funnel. *Trends Biochem.*, **2004**, *29*, 527.
5. Gregersen, N.; Bross, P.; Vang, S.; Christensen, J.H. Protein Folding and Human Disease. *Annu.Rev. Genomics Hum. Genet.*, **2006**, *7*, 103-124.
6. Galvangnion, C., Buell, A. K., Meisi, G., Michaels, T.C.T., Vendruscolo, M., Knowles, T.P.J., Dobson, C.M. Lipid Vesicles Trigger A-Synuclein Aggregation by Stimulating Primary Nucleation. *Nature chemical biology*, **2015**, *11*, 229.
7. Cohen, S. I., Linse ,S., Luheshi, L., Otzen, D.E., Vendruscolo, M., Dobson, C.M, Knowles, T.P., Proliferation of amyloid- $\beta$ 42 aggregates occurs through a secondary nucleation mechanism. *Proceeding of the National Academy of Science*, **2013**, *110*, 9758.
8. Dobson, C. M. Protein Folding and Misfolding. *Nature*, **2003**, *426*, 884.
9. Rose, G. D., Fleming, P. J., Banavar, J. R., & Maritan, A. A backbone-based Theory of Protein Folding. *Proceedings of the National Academy of Sciences*, **2016**, *103*, 16623-16633.
10. van den Berg, B., Wain, R., Dobson, C. M., & Ellis, R. J. Macromolecular Crowding Perturbs Protein Refolding Kinetics: Implications for Folding Inside the Cell. *The EMBO journal*, **2000**, *19*, 3870-3875.
11. Buxbaum, E. Fundamentals of Protein Structure and Function. *New York: Springer*, **2007**, *31*
12. Alzheimer's Association, A. S. Changing The Trajectory of Alzheimer's Disease: A National Imperative. *Washington, DC*. **2010**
13. Petanceska, S. S., DeRosa, S., Olm, V., Diaz, N., Sharma, A., Thomas-Bryant, T., ... & Refolo, L. M. Statin Therapy for Alzheimer's Disease. *Journal of Molecular Neuroscience*, **2002**, *19*, 155-161.

14. Younkin, S. G. The Role of A $\beta$ 42 in Alzheimer's Disease. *Journal of Physiology-Paris*, **1998**, *92*, 289-292.
15. Rovelet-Lecrux, A., Hannequin, D., Raux, G., Le Meur, N., Laquerrière, A., Vital, A., Dubas, F. APP Locus Duplication Causes Autosomal Dominant Early-Onset Alzheimer Disease With Cerebral Amyloid Angiopathy. *Nature genetics*, **2006**, *38*, 24.
16. LeVine III, H. Alzheimer's Disease and the  $\beta$ -amyloid Peptide. *J Alzheimers Dis*, **2010**, *19*, 311-323.
17. Mayeux, R., & Sano, M. Treatment of Alzheimer's Disease. *New England Journal of Medicine*, **1999**, *341*, 1670-1679.
18. Ohno, M., Sametsky, E. A., Younkin, L. H., Oakley, H., Younkin, S. G., Citron, M., & Disterhoft, J. F. BACE1 deficiency rescues memory deficits and cholinergic dysfunction in a mouse model of Alzheimer's disease. *Neuron*, **2004**, *41*, 27-33
19. Price, D. L., & Sisodia, S. S. Mutant Genes in Familial Alzheimer's Disease and Transgenic Models. *Annual review of neuroscience*, **1998**, *21*, 479-505.
20. Kim YT, Downs D, Wu SL, Enzymic Properties of Recombinant BACE2. *Eur J Biochem*, **2002**, *269*, 5668-77.
21. Sun, X., Wang, Y., Qing, H., Christensen, M. A., Liu, Y., Zhou, W., Liu, X. Distinct Transcriptional Regulation and Function of The Human BACE2 and BACE1 genes. *The FASEB Journal*, **2005**, *19*, 739-749.
22. Zhu, K., Peters, F., Filser, S., Herms, J. Consequences of Pharmacological BACE Inhibition on Synaptic Structure and Function. *Biological Psychiatry*. **2009**.
23. Charrier, N., Clarke, B., Demont, E., Dingwall, C., Dunsdon, R., Hawkins, J., Mosley, J. Second Generation of BACE-1 Inhibitors Part 2: Optimisation of the Non-Prime Side Substituent. *Bioorganic & medicinal chemistry letters*, **2009**, *19*, 3669-3673.
24. Mullane, K., Williams, M. Alzheimer's Therapeutics: Continued Clinical Failures Question The Validity of The Amyloid Hypothesis—But What Lies Beyond. *Biochemical pharmacology*, **2013**, *85*, 289-305.
25. Kumar, A., Srivastava, G., Srivastava, S., Verma, S., Negi, A. S., Sharma, A. Investigation of Naphthofuran Moiety As Potential Dual Inhibitor Against BACE-1 and GSK-3 $\beta$ : Molecular Dynamics Simulations, Binding Energy, and Network Analysis To Identify First-In-Class Dual Inhibitors Against Alzheimer's Disease. *Journal of molecular modeling*, **2017**, *23*, 239.

26. Shuaib, S., Goyal, B. Scrutiny of the Mechanism of Small Molecule Inhibitor Preventing Conformational Transition of Amyloid- $\beta$ 42 Monomer: Insights from Molecular Dynamics Simulations. *Journal of Biomolecular Structure and Dynamics*, **2017**, *36*, 663-678.
27. Saini, R. K., Shuaib, S., Goyal, B. Molecular Insights into A $\beta$ 42 Protofibril Destabilization With A Fluorinated Compound D744: A Molecular Dynamics Simulation Study. *Journal of Molecular Recognition*, **2017**, *30*.
28. Neill, O., Beck, E. M., Butler, C. R., Nolan, C. E., Gonzales, C., Zhang, L., Barreiro, G. Design and Synthesis of Clinical Candidate PF-06751979: A Potent, Brain Penetrant,  $\beta$ -site amyloid precursor protein cleaving enzyme 1 (BACE1) Inhibitor Lacking Hypopigmentation. *Journal of medicinal chemistry*. **2018**.
29. Mills, N. "ChemDraw Ultra 10.0" *J. Am. Chem. Soc.* *128*, 13649–13650.
30. Malde, A.K., Zuo, L., Breeze, M., Stroet, M., Poger, D., Nair, P.C., Oostenbrink, C., Mark, A.E., An Automated Force Field Topology Builder (ATB) And Repository: Version 1.0. *J. Chem. Theo. Comp.* **2011**, *17*, 4026–4037.
31. Morris, G.M., Goodsell, D.S., Halliday, R.S., Huey, R., Hart, W.E., Belew, R.K., Olson, A.J..Automated docking using a Lamarckian genetic algorithm and empirical binding free energy *J. Comput. Chem.***1998**, *19*, 1639–1662.
32. Huey, R., Morris, G.M., Olson, A.J., Goodsell. A Semi Empirical Free Energy Force Field With Charge–Based Desolvation. *J. Comput. Chem.* **2007**, *27*, 1145–1152.
33. DeLano, W.L. The PyMOL Molecular Graphics System. 571 DeLano Scientific, San Carlos, CA, USA **2002**.
34. Kumar, A., Srivastava, S., Tripathi, S., Singh, S.K., Srikrishna, S., Sharma, A., Molecular insight into amyloid oligomer destabilizing mechanism of flavonoid derivative 2-(4' W.F. van Gunsteren, H.J.C. Berendsen, A leap–frog algorithm for stochastic dynamics, *Mol. Simul.* 173–185benzyloxyphenyl)–3–hydroxy–chromen–4–one through docking and molecular dynamics simulations.*J. Biomol. Struct. Dyn.* (**2016**) *34*, 1252–1263.
35. Berendsen, H.J.C., Postma, J.P.M., Gunsteren, W.F. van., Hermans, J. Interaction Models For Water In Relation To Protein Hydration, Intermolecular Forces. *Pullman, B. (ed.), Reidel Publishing Company: Dordrecht, The Netherlands.* (**1981**) 331–342.

36. Hess, B., Bekker, H., Berendsen, H.J.C., Fraaije, J.G.E.M. LINCS: A linear Constraint Solver For Molecular Simulations. *J. Comput. Chem*, **1997**, *18*, 1463–1472.
37. ) Berendsen, H.J.C., Postma, J.P.M., van Gunsteren, W.F., DiNola, A., Haak, J.R. Molecular Dynamics With Coupling To An External Bath. *J. Chem. Phys.* **1984**, *81*, 3684–3690.
38. Essman, U., Perera, L., Berkowitz., Darden, T., Lee, H., Pedersen, L.G. A Smooth Particle Mesh Ewald Method. *J. Chem. Phys.* **1995**, *103*, 8577–8593
39. Darden, T., York, D., Pedersen, L. Particle mesh Ewald: An Nlog (N) method for Ewald sums in large systems. *J. Chem. Phys.* **1993**, *98*, 10089–10092.
40. Humphrey, W., Dalke, A., Schulten, K., VMD: Visual Molecular Dynamics *J. Mol. Graph.* **1996**, *14*, 33–38.
41. Huang, W., Lv, D., Yu, H., Sheng, R., Kim, S. C., Wu, P., Hu, Y. Dual-Target-Directed 1, 3-Diphenylurea Derivatives: BACE 1 Inhibitor And Metal Chelator Against Alzheimer's Disease. *Bioorganic & medicinal chemistry*. **2010**, *18*, 5610-5615.
42. Hamley, I. W. The amyloid beta peptide: a chemist's perspective. Role in Alzheimer's and fibrillization. *Chemical reviews*. **2012**, *112*, 5147-5192.
43. He, Y., Yao, P. F., Chen, S. B., Huang, Z. H., Huang, S. L., Tan, J. H., Huang, Z. S. Synthesis and Evaluation of 7, 8-Dehydrorutaecarpine Derivatives As Potential Multifunctional Agents For The Treatment Of Alzheimer's Disease. *European journal of medicinal chemistry*. **2013**, *63*, 299-312.
44. Welikala, R. A., Dehmeshki, J., Hoppe, A., Tah, V., Mann, S., Williamson, T. H., Barman, S. A. Automated Detection of Proliferative Diabetic Retinopathy Using A Modified Line Operator And Dual Classification. *Computer methods and programs in biomedicine*. **2014**, *114*, 247-261.
45. Zha, X., Lamba, D., Zhang, L., Lou, Y., Xu, C., Kang, D., Samez, S. Novel Tacrine–Benzofuran Hybrids As Potent Multitarget-Directed Ligands For The Treatment Of Alzheimer's Disease: Design, Synthesis, Biological Evaluation, And X-Ray Crystallography. *Journal of Medicinal Chemistry*. **2015**, *59*, 114-131.
46. Lee, W. H., Harb, J. *U.S. Patent No. 9,448,860*. Washington, DC: U.S. Patent and Trademark Office. **2016**.

47. Yan, R. Stepping Closer To Treating Alzheimer's Disease Patients With BACE1 Inhibitor Drugs. *Translational neurodegeneration*. **2016**, 5, 13.
48. Scott, J. D., Li, S. W., Brunskill, A. P., Chen, X., Cox, K., Cumming, J. N., Jiang, Q. Discovery of the 3-Imino-1, 2, 4-thiadiazinane 1, 1-Dioxide Derivative Verubecestat (MK-8931)—A  $\beta$ -Site Amyloid Precursor Protein Cleaving Enzyme 1 Inhibitor for the Treatment of Alzheimer's Disease. **2016**.
49. Timmers, M., Van Broeck, B., Ramael, S., Slemmon, J., De Waepenaert, K., Russu, A., ... & Moechars, D. Profiling the dynamics of CSF and plasma A $\beta$  reduction after treatment with JNJ-54861911, a potent oral BACE inhibitor. *Alzheimer's & Dementia: Translational Research & Clinical Interventions*. **2016**, 2, 202-212.
50. Shuaib, S., Saini, R. K., Goyal, D., Goyal, B. Insights into the Inhibitory Mechanism of Dicyanovinyl-Substituted J147 Derivative against A $\beta$ 42 Aggregation and Protofibril Destabilization: A Molecular Dynamics Simulation Study. *ChemistrySelect*. **2017**, 2, 1645-1657.
51. Kumar, S., Chowdhury, S., Kumar, S. In Silico Repurposing Of Antipsychotic Drugs For Alzheimer's Disease. *BMC neuroscience*. **2017**, 18, 76.
52. Ruderisch, N., Schlatter, D., Kuglstatter, A., Guba, W., Huber, S., Cusulin, C., Büllau, T. Potent and Selective BACE-1 Peptide Inhibitors Lower Brain A $\beta$  Levels Mediated by Brain Shuttle Transport. *EBioMedicine*. **2017**, 24, 76-92.
53. Kumar, A., Srivastava, G., Negi, A. S., Sharma, A. Docking, Molecular Dynamics, Binding Energy-MM-PBSA Studies of Naphthofuran Derivatives To Identify Potential Dual Inhibitors Against BACE-1 And GSK-3 $\beta$ . *Journal of Biomolecular Structure and Dynamics*. **2018**, 1-37.
54. Thai, N. Q., Bednarikova, Z., Gancar, M., Linh, H. Q., Hu, C. K., Li, M. S., & Gazova, Z. CID 9998128 Compound Is A Potential Multi-Target Drug For Alzheimer's Disease. *ACS Chemical Neuroscience*. **2018**.
55. Malamas, M.S., Erdei, J., Gunawan, I., Barnes, K., Johnson, M., Hui, Y., Turner, J., Hu, Y., Wagner, E., Fan, K., Olland, A., Bard, J., Robichaud, A.J. Aminoimidazoles As Potent And Selective Human B-Secretase (BACE1) Inhibitors. *J. Med. Chem.* **2009**, 52 6314-6323.

